Effective Refractive Index Approximation and Surface Plasmon Resonance Modes of Metal Nanoparticle Chains and Arrays

Ergun Simsek

Department of Electrical and Electronics Engineering, Bahcesehir University, Istanbul, Turkey

Abstract— The discrete-dipole approximation method is implemented with an effective refractive index approximation to obtain surface plasmon resonance modes of metal nanoparticle chains and arrays in a multilayered medium. This fully retarded theoretical model includes the effects of retardation, radiative damping and dynamic depolarization due to the finite size of the nanoparticles. The use of diagonal terms of dyadic Green's functions and different polarizability coefficients along the semi-axes of ellipsoidal nanoparticles provide the complete set of resonance modes. Numerical results show a reasonable agreement with experiment results.

1. INTRODUCTION

Surface Plasmons (SPs), which are simply electromagnetic waves that propagate along a conductor-dielectric interface, are quite attractive to a wide spectrum of engineers and scientists due to their potential in developing new types of optical antennas, photonic devices and sensors. Their importance comes from the fact that when periodically located, metal nanoparticles (MNPs) can lead to giant electromagnetic field enhancement and sub-wavelength lateral mode confinement.

A very important design parameter of an optical waveguide with sub-wavelength lateral mode confinement is the dispersion relation. In this direction, many researchers have studied dispersion relation of SP resonance (SPR) modes of MNP chains experimentally in the last decade [1–5]. In the mean time novel theoretical models have been developed to analyze such systems. One very commonly used theoretical model is the discrete dipole approximation (DDA) [2, 3, 6, 7]. DDA is a simple yet effective method but requires a homogeneous background that is not the case most of the time for real MNP applications, e.g., MNPs fabricated on top of indium tin oxide (ITO) coated-glass slides [1–5] creating a three-layer media (air/ITO/glass). In such structures, background can be assumed to be a multilayered environment and DDA can be still helpful given it is implemented via layered-media Green's functions (LMGFs). However, the evaluation of these computationally expensive LMGFs is a bottleneck for many researchers due to their mathematical complexity. Some researchers have tried to overcome this problem by the help of image theory (IT) [2, 7]. Experimental results support the validity of the theoretical model but it is not clear that how IT can be implemented for structures with more than two layers, especially for the case where the width of the layer (on which NPs are aligned) is less than the half of the height of the NPs.

In this work, we adopt a simple effective refractive index (ERI) approximation to overcome the above complexity issues regarding the SPR modes of metal NP chains and arrays embedded in a multilayered structure. We first applied this approximation to one dimensional (1D) periodically located NP chains. Numerical studies show that ERI results are very close to the ones obtained experimentally. Then, we applied this approximation onto two dimensional (2D) periodically located MNP arrays by extending the theory developed by Weber and Ford for the 1D case [6]. The results of this novel 2D DDA implementation show a reasonable agreement with the experiment results.

2. EFFECTIVE INDEX APPROXIMATION

In [1], Crozier et al. studies SPR modes of gold nanoparticle chains fabricated on ITO-coated glass slides. They successfully support their experimental observations by the help of numerical results obtained with a finite-difference time-domain solver, which can handle an inhomogeneous background. In that work, they also compare experimentally obtained SPR modes against numerically calculated ones based on DDA. They apply DDA technique twice: first they assume point dipoles exist in air, second they assume point dipoles exist in glass. Interestingly, experimentally obtained dispersion results lay in between those two sets of simulation results. Same research group studies the effect of ITO layer's thickness numerically in [4] and they conclude that 15 to 30 nm ITO layer causes a red shift in resonance frequencies but maintain similar characteristic in dispersion.
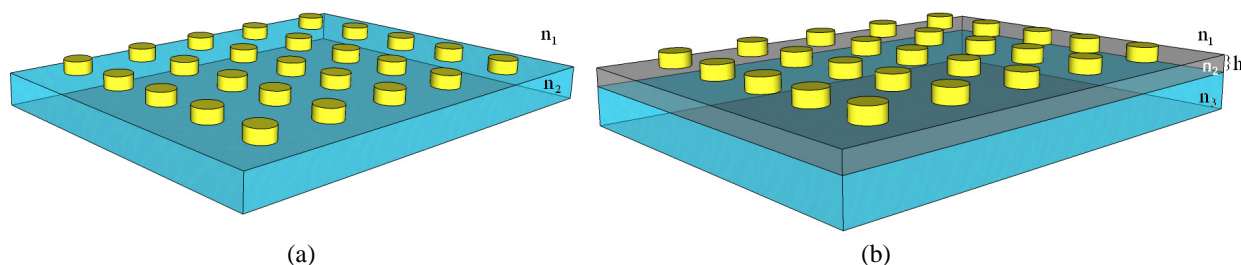
Figure 1: (a) NPs, depicted as yellow cylinders, in a two layer medium: upper layer is air; lower layer is glass, which has a thickness of several wavelengths. n_1 and n_2 are refractive indices of upper and lower layers, respectively. (b) NPs in a three layer medium, where the height of the mid-layer is h. n_1, n_2, and n_3 are refractive indices of upper, middle, and lower layers, respectively.

Inspired by these experimental studies, in this work we adopt a simple ERI model for multilayered backgrounds. We assume that a multilayered background can be replaced with a homogeneous medium whose refractive index, $n_{effective}$, depends on wavelength and each layer's refractive index, and hence we can obtain SPR modes as if MNPs are located in a homogenous medium.

We can briefly describe our ERI model as follows. If we deal with a half-space problem, depicted as Figure 1(a), we simply take the average of refractive indices of two neighboring layers. If the number of layer is more than two, ERI depends on the ratio of the width of the mid-layers to the wavelength (λ). For example, if the height of the mid-layer, h, of a three-layer background, shown as Figure 1(b), is much less than the wavelength, electric field does not propagate long enough in the mid-layer to be effected and transmitted field does not differ significantly than the one in Figure 1(a), assuming $n_1^{(a)} = n_1^{(b)}$ and $n_2^{(a)} = n_3^{(b)}$. On the other hand, if h is much larger than the wavelength, the effect of the bottom layer should be negligible. As a result of this wavelength-layer thickness dependency, the following equation is used to calculate the ERI of a three-layer medium

$$n_{effective} = \begin{cases} \dfrac{1}{2}\left[n_1 + n_2\dfrac{h}{\lambda} + \left(1 - \dfrac{h}{\lambda}\right)n_3\right], & (h \leq \lambda), \\ \dfrac{n_1 + n_2}{2}, & (h \geq \lambda). \end{cases} \tag{1}$$

It should be noted that Equation (1) simplifies into the two-layer case, when (a) h is equal to zero (b) $n_2 = n_3$ or $n_1 = n_2$. If the number of layer is more than 3, a similar methodology can be followed for each additional layer.

3. SURFACE PLASMON RESONANCE MODES

For the SPR modes of MNP chains, we follow the procedure described in [6] implemented with the ERI approximation and a comparative study is provided in Section 4. For the SPR modes of MNP arrays, we develop a novel 2D DDA method as follows.

It is known that SPR modes occur when the dipole moment of a single oscillating particle becomes equal to the induced moment. Here induced moment is defined by the sum of each surrounding particle's polarizability coefficient times the total electric field created by those surrounding oscillating dipoles. This can be written as

$$1 - \alpha_x \sum_{all} G_{xx}(x, y, z | x', y', z') = 0 \quad \text{Longitudinal mode } (L) \tag{2a}$$

$$1 - \alpha_y \sum_{all} G_{yy}(x, y, z | x', y', z') = 0 \quad \text{Transverse-1 Mode } (T_1) \tag{2b}$$

$$1 - \alpha_z \sum_{all} G_{zz}(x, y, z | x', y', z') = 0 \quad \text{Transverse-2 Mode } (T_2) \tag{2c}$$

where $G_{\xi\varphi}(x, y, z | x', y', z')$ is the Dyadic Green's function which describes the ξ-component of the electric field at (x, y, z) due to an oscillating point dipole located at (x', y', z') directing φ-axis, where ξ and φ are either x, y, or z; α_φ defines the relative polarizability along φ-axis. For a finite

number of particles, the above equations can be expressed in a matrix form, $\mathbf{S}$, as similar to the one dimensional case [6]. If we have $N \times M$ nanoparticle, $\mathbf{S}$ is an $NM \times NM$ matrix and the frequency values where determinant of $\mathbf{S}$ is equal to zero define the SP resonant modes. In order to find the complex zeros determinant of $\mathbf{S}$, we calculate the determinant of $\mathbf{S}$ on a complex radial frequency (ω) domain. The details of this complex root search will be explained at the conference.

4. NUMERICAL RESULTS

Even though we compared dozens of experiment result sets existing in the literature with the developed method, here we only provide two of them for the sake of brevity. For both, the experimental values for the optical constants of gold are used [8], rather than the Drude model to avoid the concerns about the selection of the appropriate values for plasmon and relaxation frequencies. For the simulations, the numbers of MNPs in the chain and array are equal to 20 and 400 (20×20), respectively.

4.1. One Dimensional Chain of Gold Nanoparticles

Experiment Setup: Gold NP chains are fabricated by e-beam lithography on ITO-coated glass slides [1]. The diameter and height of gold disks are 92 nm and 55 nm, respectively. Inter-particle spacing is 140 nm along the length of the chain. The thickness of ITO-coating is 20 nm. The refractive indices of ITO and air are assumed to be 1.45 and 1, respectively. The glass is assumed to be a borosilicate glass Schott BK7 (n_{BK7} changes between 1.53 and 1.51) and the ERI procedure described above is followed on the complex ω domain.

Figure 2 shows both experimental [1] and numerical results obtained via this method for the longitudinal and transverse resonant modes. Even though numerical results do not perfectly agree with the experimental results -the maximum error between them is 2.34 percent-, they still provide much closer results than the numerical results given in [1] where they use either refractive index of 1 or 1.51. The second transverse mode (T_2), depicted as the red line, agrees well with the experimental result, see [1] for details. Note that T_2 mode also interacts strongly with the light line same as the T_1 mode.

4.2. Two Dimensional Array of Gold Nanoparticles: $d_x = d_y$

Experimental Setup: Gold NP arrays are fabricated on ITO-coated glass slides with inter-particle spacing varying from 520 to 640 nm [5]. To minimize the contrast between the layers, the medium above the glass substrate is chosen to be water. The cylindrical gold disks are 180 nm in diameter and 40 nm thick. The red points in Figure 3 show resonance peak positions of the measured extinction cross section spectra as a function of grating constant. For numerical simulation, disks are approximated as ellipsoidal with semi-axes of 90, 90, and 20 nm. The refractive index of water is changes between 1.3441 and 1.326 based on the wavelength and the glass is assumed to be a
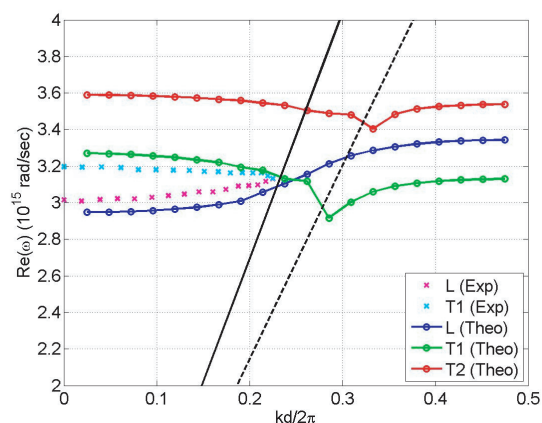
Figure 2: SP dispersion relationship of metal nanoparticle chains: experiment (dots) vs. theory (lines). Black solid and dashed lines depict the light line in air and effective medium, respectively.
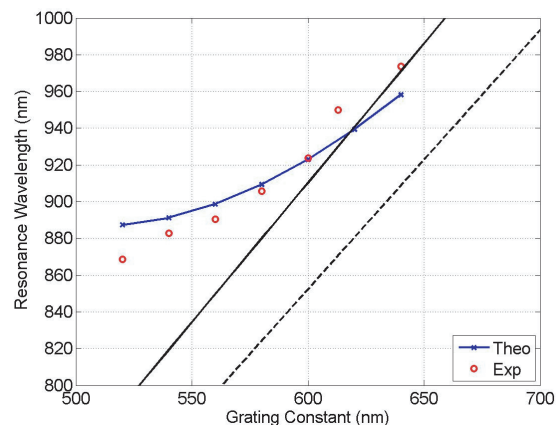
Figure 3: SPR modes of metal nanoparticle arrays: experiment (red dots) vs. theory (blue line) for $d_x = d_y = (520, 540, 560, 580, 600, 620, 640)$ nm. Black dashed and solid lines depict first grating order in glass and effective medium, respectively.

borosilicate glass Schott BK7. In Figure 3, blue solid line shows the resonant modes obtained with the 2D DDA method. Numerical results do not perfectly agree with experimental results but still provide a very good estimation: the maximum error between them is 2.25 percent. Note that there are two SPR modes due to different polarization vectors along the vertical (corresponds to T_2 mode) and horizontal axes (corresponds to L and T_1 modes, which are equivalent in this case, since interparticle spacing and semi-axes along the x and y axes are equal to each other: $d_x = d_y$ and $a = b$). Since T_2 mode occurs at wavelengths shorter than 800 nm, we do not see this mode in the figure.

5. CONCLUSIONS

Surface plasmon resonance modes of metal nanoparticle chains and arrays in a multilayered medium are approximately calculated using discrete dipole approximation method which is implemented with an effective refractive index approximation. This approximate method includes the effects of retardation, radiative damping and dynamic depolarization due to the finite size of the nanoparticles. Numerical results show that discrete dipole with effective refractive index approximation can provide a good estimate of the complete set of surface plasmon resonance modes in a multilayered medium, which might be very useful at the pre-experimental stage.

REFERENCES

1. Crozier, K., E. Togan, E. Simsek, and Y. Tang, "Experimental measurement of the dispersion relations of the surface plasmon modes of metal nanoparticle chains," *Opt. Express*, Vol. 15, 17482–17493, 2007.
2. Koenderink, A. F. and A. Polman, "Complex response and polariton-like dispersion splitting in periodic metal nanoparticle chains," *Phys. Rev. B*, Vol. 74, 033402-1-4, 2006.
3. Koenderink, A. F., R. D. Waele, J. C. Prangsma, and A. Polman, "Experimental evidence for large dynamic effects on the plasmon dispersion of sub-wavelength metal nanoparticle waveguides," *Phys. Rev. B*, Vol. 76, 201403, 1–4 Rapid Communication, 2007.
4. Yang, T. and K. B. Crozier, "Dispersion and extinction of surface plasmons in an array of gold nanoparticle chains: Influence of the air/glass interface," *Optics Express*, Vol. 16, 8570, 2008.
5. Chu, Y., E. Schonbrun, T. Yang, and K. B. Crozier, "Experimental observation of narrow surface plasmon resonances in gold nanoparticle arrays," *Appl. Physics Lett.*, Vol. 93, 181108–181111, 2008.
6. Weber, W. H. and G. W. Ford, "Propagation of optical excitations by dipolar interactions in metal nanoparticle chains," *Phys. Rev. B*, Vol. 70, 125429, 2004.
7. Noguez, C., "Surface plasmons on metal nanoparticles: The influence of shape and physical environment," *J. Phys. Chem. C*, Vol. 111, 3806–3819, 2007.
8. Rakic, A. D., A. B. Djurisic, J. M. Elazar, and M. L. Majewski, "Optical properties of metallic films for vertical-cavity optoelectronic devices," *Appl. Opt.*, Vol. 37, 5271–5283, 1998.